

# A Numerical Investigation of an Offshore Overhead Power Transmission System

Luo, Ruo

Interdisciplinary Graduate School of Engineering Sciences, Kyushu University

Zhu, Hongzhong

Research Institute for Applied Mechanics, Kyushu University

Hu, Changhong

Research Institute for Applied Mechanics, Kyushu University

<https://doi.org/10.5109/4842521>

---

出版情報 : Evergreen. 9 (3), pp.636-644, 2022-09. 九州大学グリーンテクノロジー研究教育センター  
バージョン :

権利関係 : Creative Commons Attribution-NonCommercial 4.0 International

# A Numerical Investigation of an Offshore Overhead Power Transmission System

Ruo Luo<sup>1</sup>, Hongzhong Zhu<sup>2</sup>, Changhong Hu<sup>2</sup>

<sup>1</sup>Interdisciplinary Graduate School of Engineering Sciences, Kyushu University, Fukuoka, Kasuga, 816-8580, Japan

<sup>2</sup>Research Institute for Applied Mechanics, Fukuoka, Kasuga, 816-8580, Japan

Corresponding author email: luoruo2019@riam.kyushu-u.ac.jp

(Received April 24, 2022; Revised July 11, 2022; accepted July 23, 2022).

**Abstract:** An improved numerical model is proposed to investigate the dynamics of an offshore overhead power transmission system. The hydrodynamic performance of the TLP type tower is evaluated by a potential flow theory method, and the aerodynamic performance of the electric wire is analyzed by lumped parameter method. The numerical model has been validated by comparison to water tank tests. The TLP type tower and the weight control system to reduce the body-wire interaction are newly designed for better performance in the condition of wind and wave. We found that the wire dynamics are significantly affected by the wave direction and wind direction through the numerical simulation, so the wind-wave misalignment conditions should be considered in the system safety assessment. Additionally, the safety situation of conductor wires under different environments can be studied by time-domain simulations, which can be used in system designs and feasibility discussions.

**Keywords:** Offshore overhead power transmission; Coupling analysis of TLP tower and electric wire; Safety evaluation; Wind-wave misalignment.

## 1. Introduction

Offshore wind power generation shows a potential growth at the power market in recent 10 years<sup>1)</sup>. Since systemic research and engineering development started at the beginning of this century, many countries have scheduled offshore power plants as part of their national decarbonization projects. For Japan, a country with an urgent need to confirm energy security<sup>2-4)</sup>, the government carried out laws and budgets to speed up the deployment of offshore wind power in emerging markets<sup>5)</sup>, which shows strong confidence in foresight of this industry.

Currently, submarine cables are the practical method for long-distance offshore power transmission. Though the cost of cables had been quite reduced with the development of material technology, the maintenance cost and electrical loss in transmission can reach a high level under offshore work conditions because of the complex seabed environment<sup>6-7)</sup>. As an alternative power transmission method, an offshore overhead power transmission system is proposed by our research group<sup>8)</sup>. The overview of the proposed system is shown in Fig.1, in which the tension leg platform (TLP) tower is used as the electricity transmission tower in the sea. Compared with the submarine cable method, the overhead transmission method has advantages of reducing the power transmission cost because of its relatively low

power loss and simple installation/maintenance procedure.

In this study, a hydrodynamic investigation of the offshore overhead power transmission system is carried out based on potential flow theory, and its accuracy is verified by using the data of the previous experimental study<sup>9)</sup>. Also, the TLP design is reconsidered to improve the hydrodynamics of the triangle platform in [8].

To make a comprehensive hydrodynamic evaluation of offshore structures such as floating wind turbines, we consider the wind-wave misalignment which occurs in real offshore environments<sup>10-13)</sup> in this study. This problem has also been studied in this paper for the offshore overhead power transmission system.

This paper aims to deepen the previous research and comprehensively investigate the offshore overhead power transmission system. The conductor safety is mainly considered in system evaluation for the need in practical situations. In the time-domain simulation, environmental conditions according to meteorological observations are employed to study the effect of wind-wave misalignments.

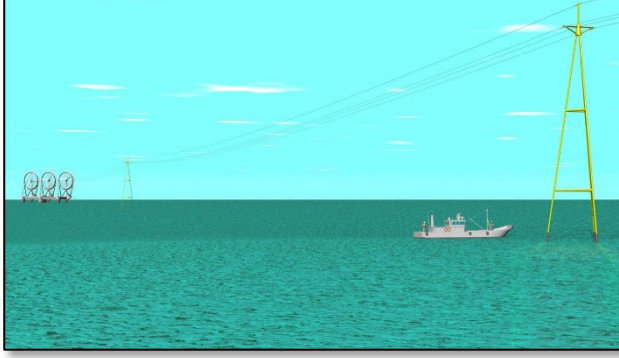


Fig.1: Overview of offshore overhead power transmission system

## 2. Numerical method

### 2.1 TLP model

Regarding the floating TLP tower as an oscillating system, the governing equation can be expressed as:

$$[M + A(\infty)]\ddot{\xi} + \int_0^t K(t - \tau)\dot{\xi}(\tau)d\tau = F \quad (1)$$

where  $M$  is the mass of TLP,  $A(\infty)$  is the added mass at infinite frequency,  $K(t)$  is the retardation function of hydro-damping. Term  $F$  is the forces including loads from wind-wave excitation, restoring forces and damping forces. The hydrodynamic force coefficients including exciting and radiation force can be obtained by potential flow programs, such as *HydroSTAR*<sup>14)</sup> or other open-sources<sup>15)</sup>, by integrating the pressure of water over the wetted surface of structure obeying potential-flow theory.

The viscous damping of TLP structure should include damping from vortex shedding in the expression of equation (1). As the potential damping can be expressed by the retardation function  $K$  mentioned above, vortex shedding damping is expressed as<sup>15)</sup>:

$$f(\dot{\xi}) = -0.5\rho C_D A |u|u \quad (2)$$

where  $A$  and  $C_D$  are the projected cross-sectional area and drag coefficient determined by Reynolds number, respectively.  $\rho$  is the water density. These damping forces and torque can also be calculated by surface integral.

Neglecting the kinetic mass of mooring lines, the hybrid linear elastic spring model<sup>16)</sup> can express the mooring forces as:

$$F_m = \begin{cases} 0 & (l_m \leq d_m) \\ k(l_m - d_m) & (l_m \geq d_m) \end{cases} \quad (3)$$

where  $l_m$  and  $d_m$  are the exact length and nominal length of tendon, respectively. By frame transformation to TLP tower, dynamic damping term  $c$  from mooring lines can be calculated as:

$$c_i = 2\zeta\sqrt{k'_i m_i} \quad (4)$$

Where  $k'_i$  is the eigen stiffness in each DOF and  $\zeta$  is the

structural damping ratio of the mooring lines.

### 2.2 Wire-tower interaction model

The conductor wire is supported by TLP towers can be regarded as a flexible line and modeled by lumped parameter system, it can be divided by several mass units connected by linear elastic units. Wire is divided into lumps of equal mass which are connected by spring-damper system to express its flexibility. A partial view of lumped-mass system can be shown in Fig.2.

On the tower top, a sheave is applied as the intermediate mechanism between the tower and conductor wires, which is shown in Fig.3. The weights, which are restricted to move along the vertical slideway, are used to strain the conductor wires. As shown in Fig.3, the mass of weights  $T$  can be adjustable by the offset  $[H_{min}, H_{max}]$  to its balance position to response to external loads.

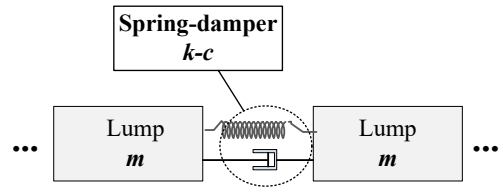


Fig.2: Wire model by lumped parameter method

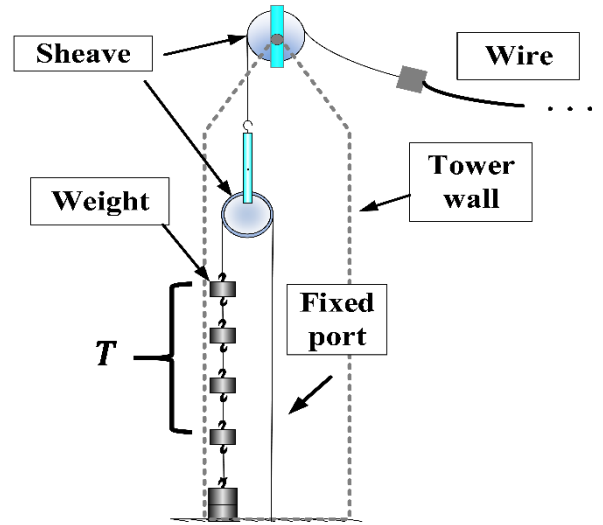


Fig.3: Sheave mechanism for conductor wires

### 2.3 Validation for numerical model

To verify the accuracy of the numerical model for the tower-wire interaction, water tank experiments<sup>9)</sup> on a TLP-wire model under regular waves were performed. The comparison of simulations and the experiment is shown in Fig.4. It is worthy to notice that the vertical axis is the ratio of wire sag  $D$  to regular wave height  $H$ . Good agreements are found in the wire motion, as shown in Fig.4. It indicates that the present numerical model is reasonably accurate in the simulation of the wire-tower interaction.

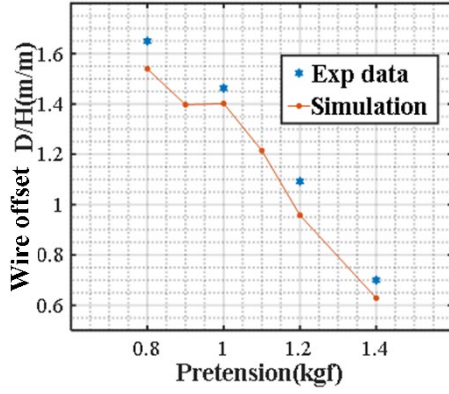


Fig.4: Comparison of wire offset

## 2.4 Wave load modeling

The real sea environment is always characterized by wave spectrums which includes various wave frequencies. In this paper, the Pierson–Moskowitz spectrum<sup>16)</sup>, which can be expressed as the following is applied to the simulation:

$$s(\omega) = C \omega^{-5} \exp(-D\omega^{-4}) \quad (5)$$

where the sea state parameters  $C$  and  $D$  are given by:

$$C = \frac{\omega_M^4 H_s^2}{4\pi} \quad D = \frac{\omega_M^4}{\pi} \quad (6)$$

where  $H_s$  and  $\omega_M$  represent the significant wave height and modal wave frequency which can be summarized from observation records, respectively. The wave excitation force respect to the wave frequencies can be calculated by:

$$F_{ex}(t) = |\Gamma(\omega)| \cdot a(\omega) \cdot \cos(\omega t + \angle\Gamma(\omega) + \varepsilon_\omega) \quad (7)$$

$$a(\omega) = \sqrt{2s(\omega)\Delta\omega} \quad (8)$$

where  $\Gamma(\omega)$  and  $\angle\Gamma(\omega)$  are the frequency-dependent amplitude and phase of the force RAOs, respectively.  $\Delta\omega$  is the constant difference between the successive frequencies in wave spectrum  $s(\omega)$ . To simulate the irregular wave environments, a random phase  $\varepsilon_\omega$  is generated by random function.

## 2.5 Wind load modeling

In the study for the interaction of wire and wind, the drag force and lift force are required. Considering the coupled motion of wire and tower can affect the aerodynamic forces, the wake oscillation model<sup>18-19)</sup> is applied to express the wind loads. Load coefficients  $C_x$ ,  $C_y$ , which are used to describe the aerodynamic loads on conductor units, can be expressed as:

$$C_x = -C_{DL} \frac{v}{u^2} \dot{y} + C_M \frac{v}{u^2} v_x - \alpha C_{DL}^2 \left(1 - \frac{\dot{x}}{u}\right) \left|1 - \frac{\dot{x}}{u}\right| \quad (9)$$

$$C_y = C_{DL} \frac{v}{u^2} (u - \dot{x}) - C_M \frac{v}{u^2} \dot{y} \quad (10)$$

$$\frac{d^2 q}{dt^2} + \epsilon \omega_s (q^2 - 1) \frac{dq}{dt} + (\omega_s^2 - \frac{\kappa}{2R} \dot{x}) q = \frac{A}{2R} \dot{y} \quad (11)$$

where  $u$  is the free wind speed along x-direction,  $v = \sqrt{(u - \dot{x})^2 + \dot{y}^2}$  is the relative velocity,  $R$  is the radius of conductor unit.  $A$ ,  $\kappa$  and  $\epsilon$  are the tuning parameters determined by wire cross-sectional shape. Considering wires of circular cross-section, dynamic lift coefficient  $C_{DL}$  and mean drag coefficient  $C_M$  can be defined as:

$$C_{DL} = 0.5qC_{L0} \quad C_M = 1.1 \quad (12)$$

Under irregular wind-wave conditions, the motion of wire is determined by the effect from both wind and TLP tower.

## 2.6 Environmental parameter

To determine the wind and wave loads used in simulations, wind-wave misalignment is important since it is common in natural sea environments. According to the histograms of misalignments of wave-wind conditions<sup>20)</sup>, the wind-wave misalignment depends on the stability of atmospheric boundary layers. The wind speed and significant wave height (SWH) in various sea states<sup>20-21)</sup> can be defined in Table 1.

$$\theta_{mis} = |\theta_{wave} - \theta_{wind}| \quad (13)$$

Table 1. Atmospheric conditions for different sea states

Sea state	Wind speed range	Average SWH	Atmospheric condition (most probable)
0~5	0~16m/s	0~5m	stable
5~8	16~30m/s	5~10m	conditional stable
8~	$\geq 30m/s$	$\geq 10m$	unstable

As shown in Table1, under the stable condition corresponding to sea level 0-5, the probability of wind-wave misalignment is almost equally distributed due to decoupled wind layers. Accordingly, the misalignment under unstable conditions highly depends on wave directions because of the turbulence in the air.

According to these facts, environmental conditions considering situations of wind farms on Japan sea<sup>22-24)</sup> are employed in numerical simulation as shown in Table 2.

As shown in Table 2, Conditions 1 and 2 correspond to a moderate situation that may happen monthly. Since the wind farm gets maximum power generation efficiency under this wind speed, both power transmission efficiency and navigation safety should be discussed in the investigation.

Condition 3 corresponds to harsh ocean environments, the sea swell reaches a high level, and the wind farm is turned to offline. Under these conditions, the safety of conductor wires should be mainly considered in the study.

Table 2. Environmental conditions in simulation

No.	Condition description			
	SWH/Period	Wind speed	Sea state	Working situation of wind farm
1	3m/8s	12m/s	4 – 5	Normal (near max output)
2	8m/11s	25m/s	7	Cut-out
3	14m/16s	50m/s	> 8	Locked

### 3. Improvement of TLP design

In this study, the design of TLP tower is improved to be able to survive in severe environmental conditions. Since the hydrodynamic performance of a TLP is mainly determined by its mooring stiffness and buoyancy, a new type TLP has been designed for easy installation in complex seabed conditions and reducing the hydrodynamics in the yaw-DOF. Three corner columns are connected to tendons, and this configuration can have less motion in yaw by dispersing the wave loads.

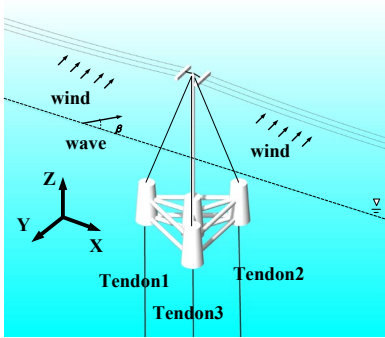


Fig.5: Overview of semi-submersible TLP

In order to avoid resonance, we improved the design by using the frequency domain analysis in practical working conditions. The natural frequency of the platform in heave, roll, and pitch should be designed in a high-frequency region, while the natural frequencies of the floating tower in the surge, sway, and yaw should be designed in a low-frequency level. The natural frequencies of TLP should satisfy:

$$\begin{aligned} (\omega_x, \omega_y, \omega_\psi) &\leq \omega_L \\ (\omega_z, \omega_\phi, \omega_\theta) &\geq \omega_H \end{aligned} \quad (14)$$

where  $x, y, \psi$  represent the motion in surge, sway and yaw,  $z, \phi, \theta$  represent the motion in heave, roll and pitch, respectively.  $[\omega_L, \omega_H]$  is the expected range of environmental wave frequencies.

Design parameters of the TLP are determined by frequency analysis under extreme environmental conditions. Since the effect of wire on TLP tower is relatively small, the pretension of wire  $T_0$  should be satisfied as below according to the TLP properties <sup>25)</sup>:

$$f_0 = \frac{\pi\sqrt{T_0/m_e}}{S_e} \geq \omega_H \quad (15)$$

$$f_{DH} = \frac{\pi\sqrt{T_E/\alpha_E m_e}}{S_e} < \min(\omega_z, \omega_\phi, \omega_\theta) \quad (16)$$

$$f_{DL} = \frac{\pi\sqrt{T_{min}/m_e}}{S_e} \geq 2\omega_M \quad (17)$$

where  $T_E$  and  $\alpha_E$  represent the tensile strength and preset safety ratio of the wire, term  $m_e$  and  $\omega_M$  are the wire's equivalent unit load in extreme wind condition and modal wave frequency in extreme condition, respectively. The stationary frequency  $f_0$  of the overhead conductor can be determined by the frequency domain shown in Fig.6. The low range  $f_{DL}$  is set as 2 times the modal frequency  $\omega_M$ , and the high range  $f_{DH}$  is set as  $\omega_z$  which is the minimum value of  $(\omega_z, \omega_\phi, \omega_\theta)$ .

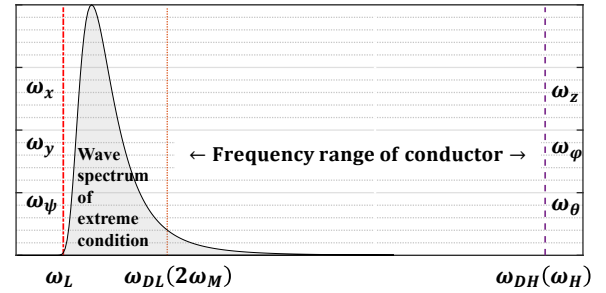


Fig.6: Frequency range considered in design

For the sheave mechanism in tower, the mass of weights  $[T_{min}, T_{max}]$  is symmetric about pretension  $T_0$ , and the value can be obtained by:

$$T_{max} = T_0 \left( 1 + \alpha_E \sqrt{\frac{m_E R_M H_M \omega_M^2}{m_e g}} \right) < 2T_0 \quad (18)$$

$$T_{min} = T_0 \left( 1 - \alpha_E \sqrt{\frac{m_E R_M H_M \omega_M^2}{m_e g}} \right) > 0 \quad (19)$$

$$\frac{T_{max}}{g} (g + R_M H_M \omega_M^2) \leq \frac{T_E}{\alpha_E} \quad (20)$$

where  $\omega_M$  and  $H_M$  is the modal wave frequency and significant wave height of extreme condition considered in the parametric design, respectively.  $T_E$  is the tensile strength of conductor.  $\alpha_E$  is the safety factor.  $R_M$  is the response amplitude operator (RAO) of TLP and can be given as equation (21):

$$R_M = \frac{|\Gamma(\omega_M)|}{\sqrt{(-\omega_M^2 m + k)^2 + [\omega_M B(\omega_M)]^2}} \quad (21)$$

where  $B$  is the added hydro damping respected to

retardation function  $K(\omega)$ .

Based on the extreme condition with an average wind speed of 60m/s and a significant wave height of 14m, the design properties of the overhead transmission system can be derived from the above assumptions and shown in Table 3.

Table 3. Design properties for the overhead power transmission system.

Property	Value
<b>TLP (tower&amp; platform)</b>	
Total mass (no water injected)	$2.12 \times 10^5 \text{kg}$
Ballast mass (fluid)	$1.60 \times 10^5 \text{kg}$
Displacement	$620 \text{m}^3$
Center of gravity (COG)	$[0, 0, -16.5] \text{(m)}$
Inertia radius	$[7.06, 7.06, 9.36] \text{(m)}$
Side-length	$20.8 \text{m}$
Tower height/ height above water	$40 \text{m}/25 \text{m}$
Natural frequencies for 6-Dofs	$[0.18, 0.18, 3.50]$ $[4.10, 4.10, 0.24] \text{ rad/s}$
Water depth	$120 \text{m}$
<b>Mooring line</b>	
Initial strain/yield strain	$0.2/0.55(\%)$
<b>Overhead conductors</b>	
Wire type	$ACSR410 \text{mm}^2$
Rated tensile strength (RTS)	$136 \text{KN}$
Stational strength	$25\% \text{RTS}$
Span	$300 \text{m}$
Stationary sag	$4.9 \text{m}$
<b>Wind</b>	
Direction	$\beta = [0^\circ, 90^\circ]$

Noticeably, columns of the platform have ballast tanks, and the TLP weight can be adjusted by ballast water. The TLP properties, such as mooring pretension and natural

frequencies, could be modified by the change of TLP weight.

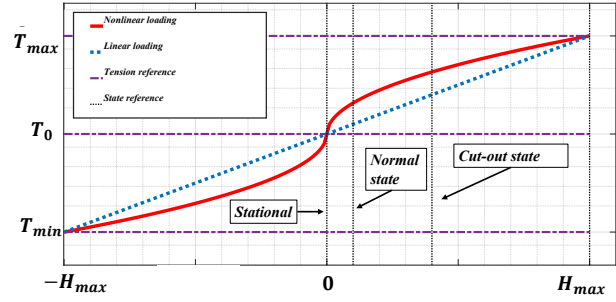


Fig.7: Fit curve of control laws in simulations, where weight mass  $T$  is mapped to its offset  $H$  ( $H = 0$ : position when system is in stationary, Reference state corresponds to  $H = R_s H_s \omega_s^2$ )

Control laws for the weight  $T$  in sheave mechanism is shown in Fig.7. The weight can be changed according to the offset  $H$  which is caused by the interaction of tower and wire. To make a contrast, control laws employed in the numerical study are set as the same limits  $[T_{min}, T_{max}]$ .

#### 4. Simulation and Evaluation under multi-directional wind-wave condition

In this section, a system including three TLP towers is employed in simulations, which can be shown in Fig.8. The towers are connected by conductor wires, and the end of conductors are connected to the substation which is regarded as a rigid point to reduce computation loads. All the results are obtained from time-domain simulations.

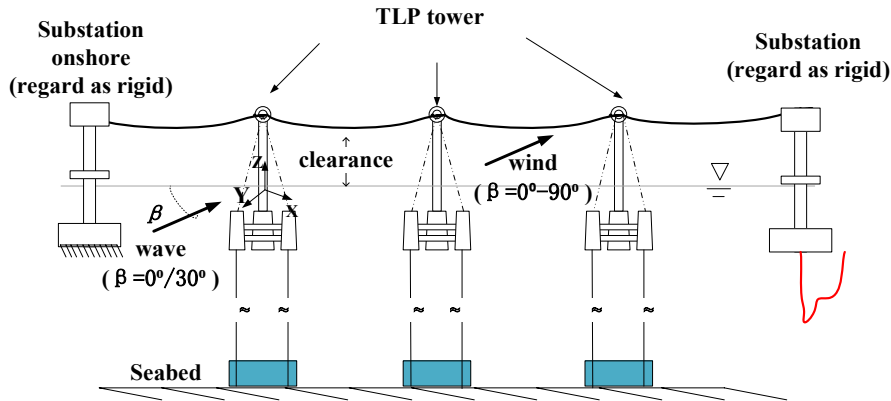


Fig.8: TLP for dynamic analysis



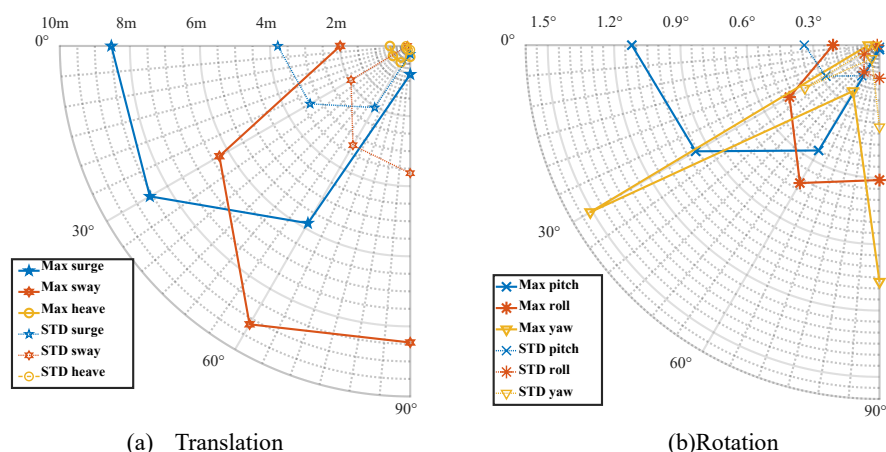


Fig.9: TLP motion in extreme waves (wave direction= $0^{\circ}$ ,  $30^{\circ}$ ,  $60^{\circ}$ ,  $90^{\circ}$ , wind direction= $90^{\circ}$ )

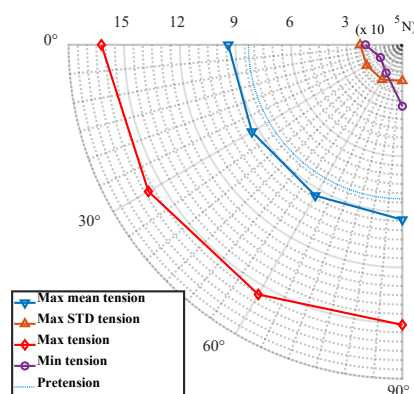


Fig.10: Tendon tension under harsh waves (wave direction= $0^{\circ}$ ,  $30^{\circ}$ ,  $60^{\circ}$ ,  $90^{\circ}$ , wind direction= $90^{\circ}$ )

#### 4.1 Hydrodynamic performance of platform

The wave of a typhoon environment (condition3 in Table 2), and wind of 50 m/s speed in the direction of  $90^{\circ}$ , are employed in the simulations to evaluate the TLP response. The motion response of the TLP can be shown in Fig.9.

As shown in Fig.9, motions of wave direction  $0^{\circ}$  and  $30^{\circ}$  have a close value of max surge offset, and yaw of TLP shows the greatest value around wave direction  $30^{\circ}$ . This may be caused by the rapid change of hydrodynamic load by the yaw motion of TLP.

The statistic characteristics of tendon tensions under extreme wave conditions are plotted in Fig.10. It can be found that the tendons will work under 200% pretension under all of wave conditions, which indicates that the design will meet the safety demand for harsh sea conditions. However, when the wave is in the direction of  $30^{\circ}$ , tension can reach a minimum value of 20% pretension. It should be noticed in practical situations since a low tension may cause destabilization (Mathieu instability) in tendons.

Since the tension of conductor wires is mainly affected by axial accelerations mainly caused by the TLP surge motion, wave directions  $0^{\circ}$  should be primarily discussed in section 4.2. The cases around sway motion

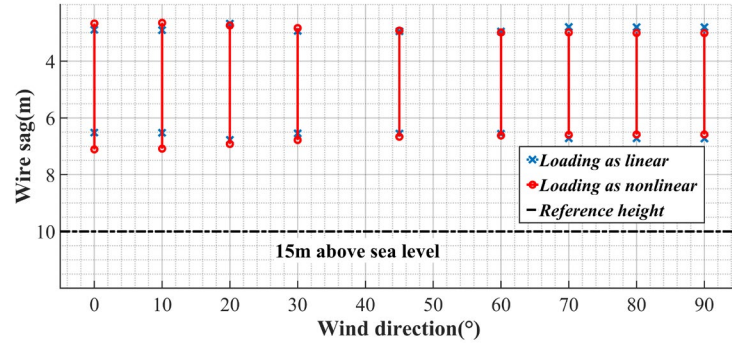
are found to have less effect on the wire.

#### 4.2 Investigation for different environmental conditions

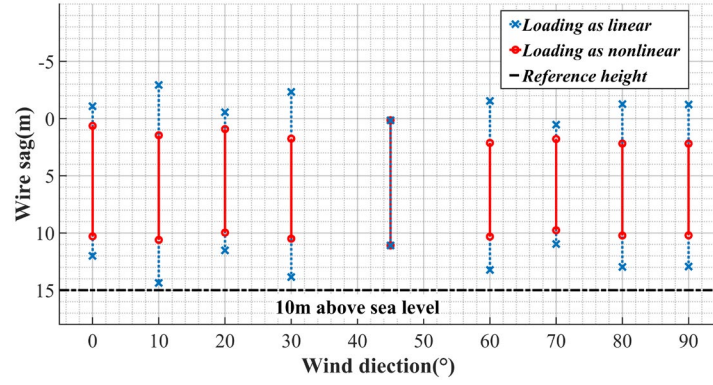
Performances of conductor wire under different environmental conditions are plotted in this section. To evaluate the power transmission efficiency and safety of ship navigation, we track the wire sag during power transmission because of its effect on the electric field distribution<sup>26)</sup>. As the suggestion of safety clearances<sup>27)</sup> for high voltage power transmission, the reference height shown in Table 4 is applied in evaluating the conductor sag in simulations. Considering the conditions of the offshore environment, we set the safety clearance as two times the reference value in Table 4 (about 15m) in the present study.

Table 4. Permissible clearance according to different voltage level in power line

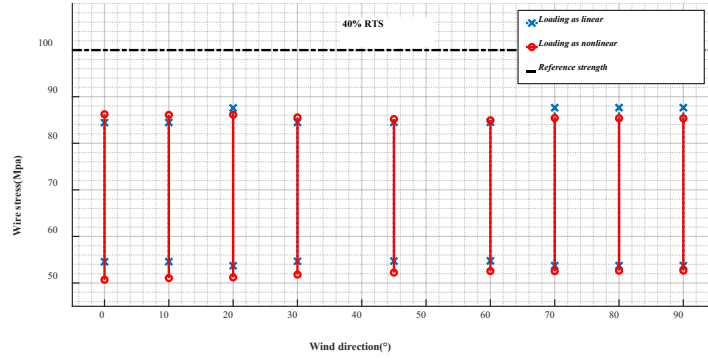
Voltage level	Vertical clearance to ground
$\leq 66KV$	6.1m
66 – 110KV	6.4m
110 – 165KV	6.7m
$\geq 165KV$	7.0m



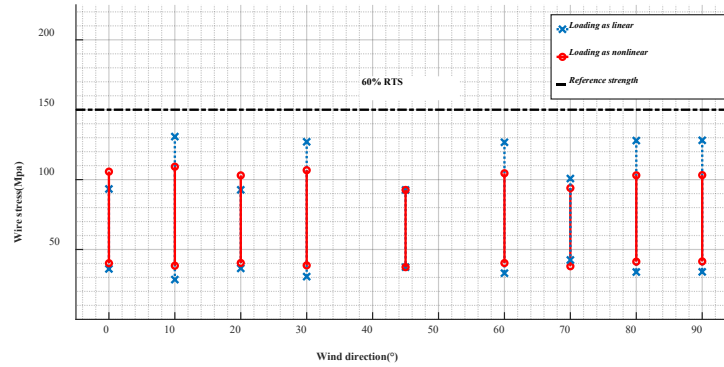
(a) Normal working condition



(b) Cut-out condition

**Fig.11:** Comparison of wire sag under working/cut-out condition in different tension-control laws (wave direction=0°)


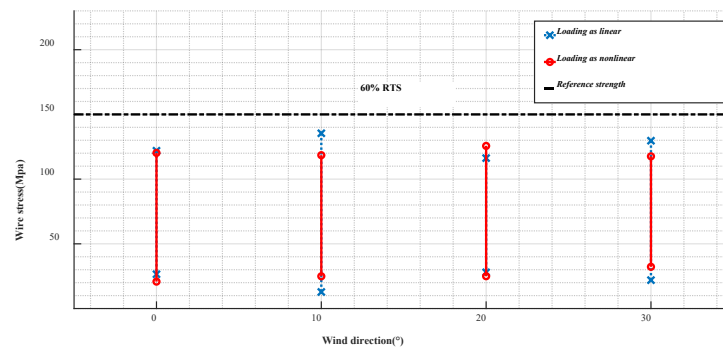
(a) normal working condition



(b) cut-out condition

**Fig.12:** Comparison of tension under normal/cut-out condition in different weight-control laws (wave direction=0°)





**Fig.13:** Comparison of tension in different weight-control laws under typhoon condition (wave direction=0°)

The situations of conductor wire under normal/harsh conditions (condition 1 and 2 in Table 2) are shown in Fig.11 and Fig.12, and baselines of reference value are used to indicate the safety situations under environmental conditions. The sag and tension of wire are significantly affected by the weight control laws. When the system employs a nonlinear law for the sheave mechanism, the upper bound of the wire sag under cut-off conditions could be limited under 11m (a height of 15m to the mean sea level), and the wire force would not exceed a value of 45% RTS. This might be caused by the more rapid weight change in the nonlinear law when the axial speed of wire reaches a maximum value around the balance position.

In addition, the tension of the conductor wire under an extreme sea environment (condition 3 in Table 2) is shown in Fig.13. The upper bound of the stress is under 60% RTS and has little difference in the two laws. The results show that the nonlinear law can improve the performance of conductor wire under cut-out conditions without significant change under other conditions, which indicates more acceptable in practical situations compared to linear law.

## 6. Conclusion

In this paper an improved numerical model is proposed to investigate the dynamics of an offshore overhead power transmission system. The hydrodynamic performance of the TLP type tower is evaluated by a potential flow theory method, and the aerodynamic performance of the overhead electric wire is analyzed by lumped parameter method. The effect of wind-wave misalignment is numerically studied. The safety factors of conductor wires are discussed through time-domain simulations, which are made under conditions based on the real sea environments. Major findings of the present study can be summarized as follows:

- Lumped parameter method can model the interaction of tower and wire dynamic in an acceptable simulate accuracy through the validation.
- The improved TLP system design has been evaluated for various sea environments, including wind-wave conditions. The results show that the most dangerous situation of mooring lines may occur at the wave

direction 30° because of a minimum tension.

- The employment of weight control scheme may significantly influence the conductor wire in sea environments. Compared to the linear control, the use of nonlinear weight control can significantly reduce the wire motion under a cut-out condition, which can improve the stability of overhead power transmission system in harsh sea environments.

## Reference

- 1) <https://www.ren21.net/reports>. *Renewables 2021 Global Status Report*, (2021)153-158
- 2) Munim Kumar Barai, Bidyut Baran Saha. Energy Security and Sustainability in Japan. *Evergreen*, **vol.2(01)**, (2015)49-56
- 3) Kana Moroga, Akiya Nagata, Yasutaka Kuriyama, Toshiya Kobayashi, Koichi Hasegawa. State of Implementation of Environmental and Energy Policies Adopted by the Regional Governments in Japan. *Evergreen*, **vol.2(02)**, (2015)14-23
- 4) Hiroki Gima, Tsuyoshi Yoshitake. A Comparative Study of Energy Security in Okinawa Prefecture and the State of Hawaii. *Evergreen*, **vol.3(02)**, (2016)36-44
- 5) Yoshinori Ueda. The Recent Offshore Wind Power Development. *Journal of the Japan Institute of Energy*, **vol.97**, (2018)125-134
- 6) LIU Gang, CAO Jingying, LU Ying. Selection Criteria of High-voltage Submarine Cables for Offshore Wind Farms by Life Cycle Cost. *High Voltage Engineering*, **vol.41**, (2015)2674-2680.
- 7) Kristen R. Schell, João Claro, Seth D. Guikema. Probabilistic cost prediction for submarine power cable projects, *Electrical Power and Energy Systems*, **vol.90**, (2017) 1–9
- 8) H. Zhu, C.Hu. A Study on Floating Overhead Power Transmission System for Offshore Energy Development: Design, Modeling and Numerical Analysis. *Ocean Engineering*, 236(2021)109528
- 9) Hongzhong Zhu, Ruo Luo, Changhong Hu, Joshiro Noda. An Experimental Study on Tower-Wire Interaction for Offshore Overhead Power

- Transmission Concept. *The autumn meeting of The Japan Society of Naval Architects and Ocean Engineers (JASNAOE)*, 2020.
- 10) Lucie Barj, Jason M. Jonkman, Amy Robertson ,etc. Wind-Wave Misalignment in the Loads Analysis of a Floating Offshore Wind Turbine. *32nd ASME Wind Energy Symposium*, 2014.
- 11) Erin E. Bachynski, Marit I. Kvittem, Chenyu Luan, Torgeir Moan. Wind-Wave Misalignment Effects on Floating Wind Turbines: Motions and Tower Load Effects. *Journal of Offshore Mechanics and Arctic Engineering*, **vol.136**, Issue 4, (2014).
- 12) C. Sun, V. Jahangiri. Bi-directional vibration control of offshore wind turbines using a 3D pendulum tuned mass damper. *Mechanical Systems and Signal Processing*, **vol.105**, (2018)338-360.
- 13) Tim Fischer, Patrick Rainey, Ervin Bossany, Martin Kühn. Study on control concepts suitable for mitigation of loads from misaligned wind and waves on offshore wind turbines supported on monopiles. *Wind Engineering*, **vol. 35**, No.5. (2011)561-574.
- 14) Bureau Veritas. *Hydrostar for expert's user manual*, <https://www.docenti.unina.it/webdocenti-be/allegati/materiale-didattico/576434>. [accessed on 26/April/2019] (2016).
- 15) Liu. Y. HAMS: a frequency-domain preprocessor for wave-structure interactions— theory, development, and application. *Journal of Marine Science and Engineering*, 7(3), (2019), 81.
- 16) T. I. Fossen. *Handbook of marine craft hydrodynamics and motion control*, John Wiley & Sons, (2011).
- 17) Y. M. Low. Frequency domain analysis of a tension leg platform with statistical linearization of the tendon restoring forces. *Marine Structures*, **vol.22** (2009) 480-503.
- 18) M.L. Facchinetti, E. de Langrea, F. Biolley. Coupling of structure and wake oscillators in vortex-induced vibrations, *Journal of Fluids and Structures*, **vol.19**, (2004) 123-140
- 19) Yang Qu, Andrie. V. Metrikine. A single van der pol wake oscillator model for coupled cross-flow and in-line vortex-induced vibrations, *Ocean Engineering*, **vol.196**, (2020).
- 20) Barth, S, Eecen, P.J, Description of the Relation of Wind, Wave and Current Characteristics at the Offshore Wind Farm Egmond Aan Zee(OWEZ) Location in 2006. ECN (2007). Technical Report No. ECN-E-07-104.
- 21) Faltinsen. O. M. *Sea loads on ships and offshore structures*. Cambridge University Press (1990)
- 22) Shigeo Yoshida, Tomoaki Utsunomia, Effects of Wave –Wind Directional Misalignment on Dynamic Characteristics and Fatigue Loads of Spar-type Floating Offshore Downwind Turbine. *Japan society of Mechanical Engineering (JSME) Fluids Engineering Conference 2010*.
- 23) Hajime Mase, Ryo Tanaka, Nobuhito Mori, Tomohiro Yasuda. Long-term Variability of Annual Large Waves along Coasts of the Sea of Japan. *Japan Society of Civil Engineering (JSCE)*, **vol.B2-65**,(2009)1251-1255.
- 24) Hye-Jin Wooa, Kyung-Ae Park. Long-term trend of satellite-observed significant wave height and impact on ecosystem in the East/Japan Sea. *Deep Sea Research Part II: Topical Studies in Oceanography*. **vol.143**, (2017) 1-14.
- 25) M Irvine. *Cable Structures*, Dover Publications, 1992.
- 26) Adel Z. El Dein, Mohamed A. A. Wahab. The Effects of the Span Configurations and Conductor Sag on the Electric-Field Distribution Under Overhead Transmission Lines. *IEEE Transactions on Power Delivery*, **vol.25**, no.4(2010)2891-2902.
- 27) F. Oluwajobi, O. Ale. Effect of sag on transmission line. *Journal of Emerging Trends in Engineering and Applied Sciences*, **vol.3**, no. 4(2012) 627-630.